

# Hypoxia-inducible factors mediate coordinated RhoA-ROCK1 expression and signaling in breast cancer cells

Daniele M. Gilkes<sup>a,b,c</sup>, Lisha Xiang<sup>a,b</sup>, Sun Joo Lee<sup>a,b</sup>, Pallavi Chaturvedi<sup>a,b</sup>, Maimon E. Hubbi<sup>a,b</sup>, Denis Wirtz<sup>c,d</sup>, and Gregg L. Semenza<sup>a,b,c,e,f,g,h,i,1</sup>

<sup>a</sup>Vascular Program, Institute for Cell Engineering, <sup>b</sup>McKusick–Nathans Institute of Genetic Medicine, and Departments of <sup>e</sup>Pediatrics, <sup>f</sup>Oncology, <sup>g</sup>Medicine, <sup>h</sup>Radiation Oncology, and <sup>i</sup>Biological Chemistry, The Johns Hopkins University School of Medicine, Baltimore, MD 21205; and <sup>c</sup>Johns Hopkins Physical Sciences-Oncology Center and <sup>d</sup>Department of Chemical and Biomolecular Engineering, The Johns Hopkins University, Baltimore, MD 21218

Contributed by Gregg L. Semenza, November 19, 2013 (sent for review October 7, 2013)

**Overexpression of Rho kinase 1 (ROCK1) and the G protein RhoA is implicated in breast cancer progression, but oncogenic mutations are rare, and the molecular mechanisms that underlie increased ROCK1 and RhoA expression have not been determined. RhoA-bound ROCK1 phosphorylates myosin light chain (MLC), which is required for actin-myosin contractility. RhoA also activates focal adhesion kinase (FAK) signaling. Together, these pathways are critical determinants of the motile and invasive phenotype of cancer cells. We report that hypoxia-inducible factors coordinately activate RhoA and ROCK1 expression and signaling in breast cancer cells, leading to cell and matrix contraction, focal adhesion formation, and motility through phosphorylation of MLC and FAK. Thus, intratumoral hypoxia acts as an oncogenic stimulus by triggering hypoxia-inducible factor → RhoA → ROCK1 → MLC → FAK signaling in breast cancer cells.**

cytoskeletal reprogramming | metastasis | migration | oxygen | tumor microenvironment

Invasion and metastasis are complex processes leading to dissemination of cancer cells from the primary tumor to distant organs. A critical step is cytoskeletal reprogramming, which transforms rigid, immobile epithelial cells to motile, invasive cancer cells. Members of the Rho family of GTPases play a central role in this process by functioning as molecular switches that control morphogenesis and movement (1). Rho proteins mediate both polymerization of actin (F-actin formation) to create stress fibers, which are antiparallel actin filaments that are crosslinked by myosin, and activation of myosin to trigger contractility (2, 3). Active (GTP-loaded) Rho binds to Rho-associated coiled-coil-forming kinase (ROCK), resulting in activation of the kinase (4). This activation mediates the phosphorylation of myosin light chain (MLC) as well as indirectly by inhibiting myosin phosphatase (MYPT), leading to actin-myosin contraction (5, 6). ROCK also phosphorylates LIM kinase, which inhibits actin depolymerization (7).

For cells to move, force generated by actin-myosin contractility is used to pull on the extracellular matrix (ECM) at focal adhesions, and ECM stiffness promotes the formation of focal adhesions (8). Conversely, substrate stiffness is induced by cell contraction and leads to the activation of focal adhesion kinase (FAK), which is required for mechanosensing and cell motility (9–11). A positive regulatory loop exists between Rho family member A (RhoA) and FAK signaling. In mouse models, FAK plays a critical role in breast cancer progression (12, 13).

*ROCK1* and *RHOA* gene expression are coordinately up-regulated in motile cells isolated from metastatic breast cancers (14). Clinical and experimental data indicate that increased expression of RhoA or ROCK1 is associated with breast cancer progression (15–19). Somatic mutations do not account for RhoA or ROCK1 overexpression in the majority of breast cancers, and the underlying molecular mechanisms remain undefined.

The presence of intratumoral hypoxia, i.e., reduced O<sub>2</sub> availability within cancer as compared with normal tissue, is associated

with an increased risk of invasion and metastasis (20–23). Cancer cells respond to the hypoxic microenvironment through the activity of hypoxia-inducible factors 1 (HIF-1) and 2 (HIF-2). HIFs are transcription factors that are composed of an O<sub>2</sub>-regulated HIF-1 $\alpha$  or HIF-2 $\alpha$  subunit and a constitutively expressed HIF-1 $\beta$  subunit (24). We used genetic and pharmacologic loss-of-function studies in mouse models to demonstrate that HIF-1, HIF-2, or both activate the transcription of a battery of genes whose protein products are required for discrete steps in the process of breast cancer invasion and metastasis via lymphatic and blood vessels (25–29). In primary tumor biopsies, elevated HIF-1 $\alpha$  protein levels are associated with an increased risk of metastasis and mortality that is independent of breast cancer grade or stage (30–33). Increased HIF-2 $\alpha$  levels also are associated with cancer progression (34).

Given the essential role of HIFs and the RhoA–ROCK1 pathway in breast cancer invasion, we hypothesized that the motility of breast cancer cells may be enhanced under hypoxic conditions by a molecular mechanism involving interplay between these two pathways. Our studies revealed that HIFs regulate RhoA and ROCK1 expression and activity directly, as determined by MYPT and MLC phosphorylation in vitro and in vivo. HIF-dependent RhoA–ROCK1 signaling resulted in cell contraction, cell-induced matrix contraction, formation of focal adhesions, FAK activation, and increased cell motility. The coordinate activation of *RHOA* and *ROCK1* expression by HIFs was associated with decreased survival of breast cancer patients. Taken together, these results provide a molecular mechanism by which intratumoral hypoxia activates a critical signal-transduction pathway that is required for breast cancer motility, invasion, and metastasis.

## Significance

Breast cancers often contain regions of reduced O<sub>2</sub> availability, leading to increased activity of hypoxia-inducible factors (HIFs). Here, we demonstrate that HIFs activate transcription of the Rho family member *RHOA* and Rho kinase 1 (*ROCK1*) genes, leading to cytoskeletal changes that underlie the invasive cancer cell phenotype. *ROCK1* is a kinase that regulates myosin light-chain activity, leading to actin-myosin contraction, which is the basis for cell movement. Coordinately increased levels of RhoA and ROCK1 mRNA in human breast cancers predicted patient mortality. These results demonstrate that a microenvironmental stimulus, hypoxia, can activate a critical signal transduction pathway, independent of genomic alterations, to drive cancer progression.

Author contributions: D.M.G. and G.L.S. designed research; D.M.G., L.X., S.J.L., P.C., and M.E.H. performed research; D.W. contributed new reagents/analytic tools; D.M.G. and G.L.S. analyzed data; and D.M.G. and G.L.S. wrote the paper.

The authors declare no conflict of interest.

See Commentary on page 887.

<sup>1</sup>To whom correspondence should be addressed. E-mail: gsemenza@jhmi.edu.

This article contains supporting information online at [www.pnas.org/lookup/suppl/doi:10.1073/pnas.1321510111/-DCSupplemental](http://www.pnas.org/lookup/suppl/doi:10.1073/pnas.1321510111/-DCSupplemental).

## Results

**HIFs Mediate Increased Cell Motility, Formation of Stress Fibers, and Matrix Contraction in Hypoxic Breast Cancer Cells.** Cell motility is a necessary prerequisite for tissue invasion (35). Previous studies have examined the influence of hypoxia on cell motility using Boyden chamber assays, which do not permit dynamic or single-cell resolution and are confounded by the influence of gravitational force and pore size. Other studies have used video microscopy to examine breast cancer cells that were exposed to hypoxia, replated, and analyzed for short (20-min) periods of time (36). We previously generated MDA-MB-231 subclones, which were stably transfected with an empty vector (shEV) or expression vectors encoding shRNA targeting both HIF-1 $\alpha$  and

HIF-2 $\alpha$  (sh1/2 $\alpha$ ), and found that the sh1/2 $\alpha$  subclone showed impaired lymphatic and vascular metastasis after injection into the mammary fat pad (29, 37). There was no difference in the viability of the two MDA-MB-231 subclones under either 20% or 1% O<sub>2</sub> (29). We dynamically monitored the random motility of shEV and sh1/2 $\alpha$  cells exposed to 20% or 1% O<sub>2</sub> on collagen-coated surfaces for 22 h. Mean cell velocity determined at 4-h intervals revealed increased velocity starting at 14 h of exposure to 1% O<sub>2</sub>, whereas cells exposed to 20% O<sub>2</sub> retained a constant velocity throughout the experiment (Fig. 1*A* and *Movies S1–S4*). Hypoxia-induced increases in cell velocity were HIF dependent and led to an increase in the maximum displacement of cells from their origin (Fig. 1*A* and *B*). The time-lapse movies revealed that the morphology of the MDA-MB-231 sh1/2 $\alpha$  subclone was

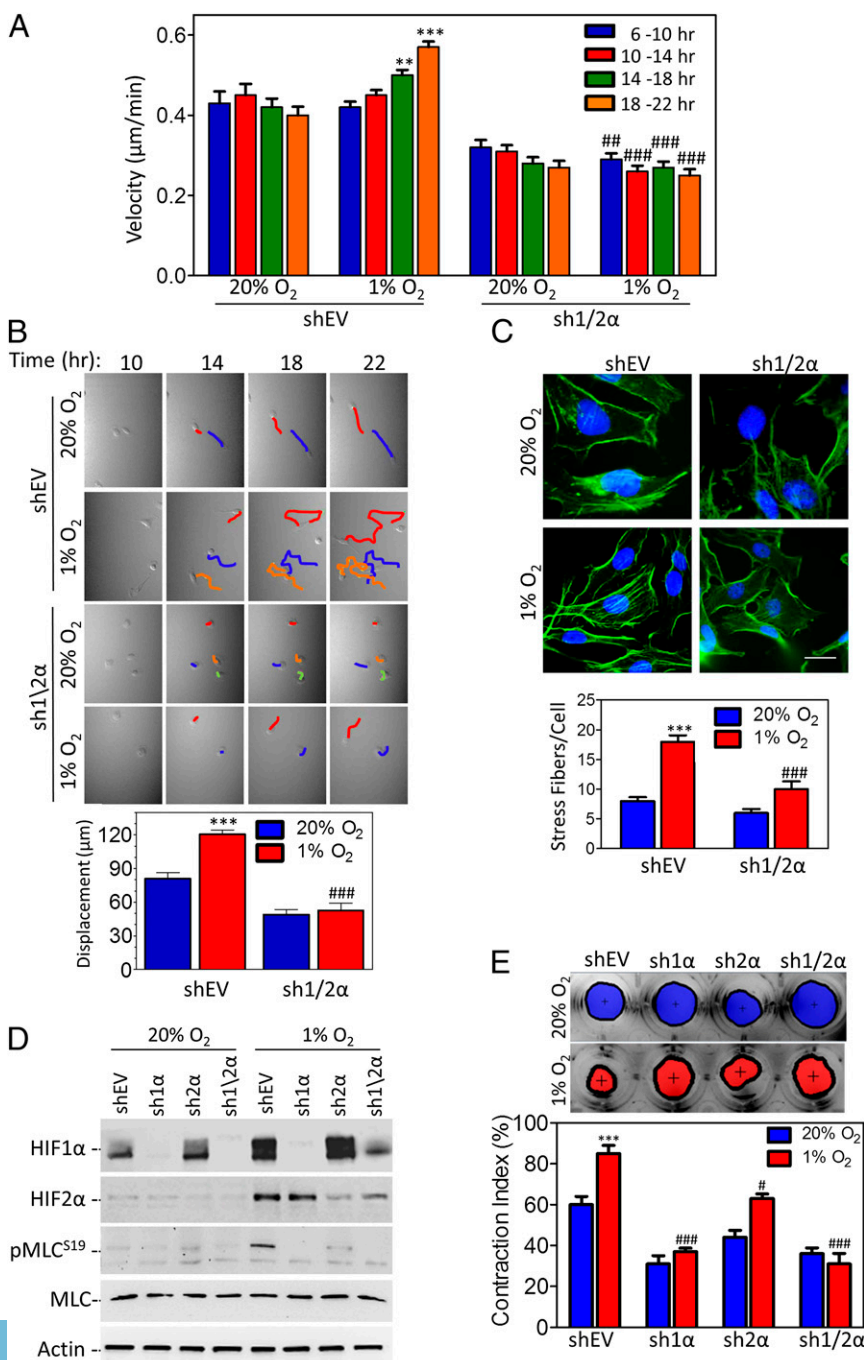


**Fig. 1.** HIFs mediate increased cell motility, the formation of stress fibers, and matrix contraction by hypoxic breast cancer cells. (A) Cell velocity over 4-h intervals was determined for MDA-MB-231 subclones, which were stably transfected with empty vector (shEV) or expression vectors encoding shRNA against HIF-1 $\alpha$  and HIF-2 $\alpha$  (sh1/2 $\alpha$ ), plated on a 2D collagen-coated substratum, and exposed to 20% or 1% O<sub>2</sub> for 22 h. Data shown are mean  $\pm$  SEM;  $n = 50$  cells;  $^{*}P < 0.01$ ,  $^{***}P < 0.001$  vs. shEV cells at 20% O<sub>2</sub> at the corresponding time point;  $^{*}P < 0.01$ ,  $^{***}P < 0.001$  vs. shEV cells at 1% O<sub>2</sub> at the corresponding time point (two-way ANOVA with Bonferroni posttest). (B) (Upper) Representative cell trajectories are shown for the indicated subclone, O<sub>2</sub> concentration, and time point. (Lower) Maximum displacement from the origin (mean  $\pm$  SEM) was determined for cells analyzed in A.  $^{***}P < 0.001$  vs. shEV cells at 20% O<sub>2</sub>;  $^{***}P < 0.001$  vs. shEV cells at 1% O<sub>2</sub> (two-way ANOVA with Bonferroni posttest). (C) (Upper) MDA-MB-231 subclones were exposed to 20% or 1% O<sub>2</sub> for 24 h and stained with FITC-conjugated phalloidin (green) to detect F-actin (stress fibers) and with DAPI to detect nuclei (blue). (Lower) The number of stress fibers per cell is shown. Data are shown as mean  $\pm$  SEM;  $n = 10$  cells.  $^{***}P < 0.001$  vs. shEV cells at 20% O<sub>2</sub>;  $^{***}P < 0.001$  vs. shEV cells at 1% O<sub>2</sub> (two-way ANOVA with Bonferroni posttest). (D) Immunoblot assays were performed to quantify levels of HIF-1 $\alpha$ , HIF-2 $\alpha$ , total MLC, pMLC<sup>S19</sup>, and actin following exposure to 20% or 1% O<sub>2</sub> for 24 h. (E) (Upper) Area of MDA-MB-231 cell-embedded collagen gels following exposure to 20% or 1% O<sub>2</sub> for 18 h. (Lower) The contraction index was calculated as  $A(t_0) - A(t_{18})/A(t_0) \times 100\%$  where  $A(t_0)$  and  $A(t_{18})$  are the gel area at the start and the end of the experiment, respectively. Data are shown as mean  $\pm$  SEM;  $n = 3$  gels.  $^{***}P < 0.001$  vs. shEV cells at 20% O<sub>2</sub>;  $^{***}P < 0.001$ ,  $^{*}P < 0.05$  vs. shEV cells at 1% O<sub>2</sub> (two-way ANOVA with Bonferroni posttest).

rounded and lacked the protrusions indicative of a motile cell phenotype that were noted in the shEV subclone.

Increased formation of actin stress fibers and enhanced contractility are common features of motile cells in 2D culture conditions (38). Immunofluorescent staining of polymerized actin (F-actin) using FITC-conjugated phalloidin revealed an HIF-dependent increase in the formation of stress fibers following exposure of cells to hypoxic conditions for 24 h (Fig. 1C).

Cells make attachments to the ECM at focal adhesion sites and transmit contractile forces to the substratum via actin stress fibers. MLC phosphorylation on serine-19 (pMLC<sup>S19</sup>) is required to coordinate the formation of stress fibers. To determine the individual and joint contribution of HIF-1 $\alpha$  and HIF-2 $\alpha$  to the regulation of MLC phosphorylation, MDA-MB-231 subclones transduced with expression vectors encoding shRNA targeting either HIF-1 $\alpha$  (sh1 $\alpha$ ) or HIF-2 $\alpha$  (sh2 $\alpha$ ) were also established (29). The levels of pMLC<sup>S19</sup> were increased significantly in the shEV subclone following 24-h exposure to 1% O<sub>2</sub> (Fig. 1D). Knockdown of HIF-1 $\alpha$  completely abrogated and HIF-2 $\alpha$  knockdown significantly reduced pMLC<sup>S19</sup> induction by hypoxia. The impaired hypoxia-induced MLC phosphorylation was associated with absent or reduced ability, respectively, of sh1 $\alpha$  and sh2 $\alpha$  subclones to induce matrix contraction when embedded in type I collagen (Fig. 1E). This finding was recapitulated in fibroblasts transduced with the same shRNA vectors (Fig. S1), suggesting that intratumoral hypoxia also may induce HIF-dependent cytoskeletal changes in stromal cells and demonstrating that these responses are not dependent on somatic mutations present in breast cancer cells. Taken together, the data presented in Fig. 1 demonstrate that inhibition of HIFs decreases cell motility, the formation of stress fibers, MLC phosphorylation, and cell-induced ECM contraction in response to hypoxia.

**Increased RhoA and ROCK1 Expression and Activity in Hypoxic Breast Cancer Cells.** RhoA-bound ROCK1 phosphorylates and inhibits MYPT; it also directly phosphorylates and activates MLC, resulting in increased levels of pMLC<sup>S19</sup>. To determine whether RhoA or ROCK1 plays a role in hypoxia-induced MLC activation, RhoA and ROCK1 mRNA and protein levels were analyzed in cells exposed to 20% or 1% O<sub>2</sub> (Fig. 2A and B). Quantitative real-time RT-PCR (qRT-PCR) revealed that RhoA and ROCK1 (but not ROCK2) mRNA levels increased under hypoxic conditions in a panel of nontumorigenic (MCF10A), tumorigenic but non-metastatic (MCF-7 and T47D), and metastatic (MDA-MB-231 and MDA-MB-435) breast cell lines (Fig. 2A and Fig. S2). RhoA and ROCK1 protein levels also increased modestly after 48 h at 1% O<sub>2</sub> and were associated with MYPT phosphorylation at threonine-853, which is a ROCK1-specific phosphorylation site that inhibits MYPT activity. pMLC<sup>S19</sup> was enhanced in T47D, MDA-MB-231, and MDA-MB-435 cells under hypoxic conditions but was not detectable in MCF10A or MCF-7 cells cultured under either 20% or 1% O<sub>2</sub> (Fig. 2B). Overall, the magnitude of RhoA and ROCK1 expression correlated with the metastatic potential of the cell lines, as is consistent with studies in mouse models showing that RhoA and ROCK1 are required for breast cancer metastasis (16, 18, 39).

To determine the clinical relevance of RhoA and ROCK1 overexpression in human breast cancer, survival data from two independent cohorts (40, 41) were analyzed by stratifying patients according to RhoA, ROCK1, ROCK2, or combined RhoA and ROCK1 mRNA levels in the primary tumor (Fig. 2C and D). ROCK2 mRNA expression, which was not induced by hypoxia (Fig. S2A), did not correlate with patient survival in either dataset. ROCK1 mRNA levels also were not significantly associated with survival. In contrast, RhoA mRNA levels above the median were associated with decreased patient survival. The most significant difference in survival was observed when patients who expressed high levels (above the median level of expression) of both RhoA

and ROCK1 mRNA in their primary tumor were compared with patients who expressed low levels of both mRNAs. Taken together, the data presented in Fig. 2 show that RhoA and ROCK1 mRNA and protein expression are coordinately induced by hypoxia and that combined overexpression predicts mortality of breast cancer patients.

#### Hypoxia-Induced RhoA and ROCK1 Expression Is HIF Dependent.

Gene-expression data from 597 breast cancers (42) was used to compare levels of RhoA and ROCK1 mRNA with expression of prolyl 4-hydroxylase, alpha polypeptide I (P4HA1), P4HA2, VEGF, LOX, PLOD1, and ANGPTL4 mRNA, which are HIF regulated in breast cancer cells. RhoA and ROCK1 mRNA levels were significantly correlated with five of the six HIF target genes analyzed, unlike ROCK2 mRNA (expression of which is not regulated by hypoxia or HIFs) (Fig. S3A and B). As a positive control, the expression of *LICAM* (another known HIF target gene) was analyzed; its expression also was correlated with five of the six HIF target genes (Fig. S3A). These data provide evidence for HIF-dependent RhoA and ROCK1 expression in human breast cancers.

In MDA-MB-231 cells, an increase in RhoA and ROCK1 protein levels occurred following 12 h of hypoxic exposure and continued for at least 48 h (Fig. S3C). The hypoxic induction of RhoA and ROCK1 mRNA and protein was inhibited significantly in the sh1 $\alpha$ , sh2 $\alpha$ , and sh1/2 $\alpha$  subclones (Fig. 3A and B and Fig. S3D). The knockdown of HIF-1 $\alpha$  or HIF-2 $\alpha$  blocked ROCK1-dependent phosphorylation of MYPT (at T853 and T696, which are also ROCK-dependent phosphorylation sites) and MLC (at S19) under hypoxic conditions in MDA-MB-231 cells (Fig. 3B) and fibroblasts (Fig. S3E). Furthermore, exposure of breast cancer cells to hypoxia was sufficient to induce HIF-dependent activation of RhoA, as measured by a specific Rho-GTP binding assay, without the addition of growth factors (Fig. 3C).

To assess RhoA and ROCK1 expression in vivo, MDA-MB-231 shEV and sh1/2 $\alpha$  subclones were injected orthotopically into the mammary fat pad of immunodeficient mice, and tumors were harvested on day 52. We have reported previously that primary tumor growth and metastasis of the sh1/2 $\alpha$  subclone to lymph nodes and lungs was reduced significantly relative to the shEV subclone (29, 37). RhoA and ROCK1 mRNA levels were decreased significantly in tumors derived from sh1/2 $\alpha$  as compared with shEV subclones; this decrease was comparable to the reduced expression of HIF-1 $\alpha$  and P4HA1 mRNA (Fig. 3D). Immunohistochemistry revealed intense nuclear HIF-1 $\alpha$  staining in perinecrotic (hypoxic) regions of shEV tumors (Fig. 3E) but not in sh1/2 $\alpha$  tumors (Fig. S3F). Analysis of adjacent shEV tumor sections revealed increased RhoA and ROCK1 expression that colocalized with HIF-1 $\alpha$  in perinecrotic regions (Fig. 3E, *Bottom Row*). Taken together, the data presented in Fig. 3 demonstrate that HIFs mediate the coordinate expression of RhoA and ROCK1 in hypoxic breast cancer cells both in vitro and in vivo.

**RHOA and ROCK1 Are Direct HIF Target Genes.** The human *RHOA* and *ROCK1* genes were searched for matches to the consensus HIF binding site sequence 5'-(A/G)CGTG-3' (43). Seven candidate sites in the *RHOA* gene and nine candidate sites in the *ROCK1* gene were interrogated by ChIP assays of MDA-MB-231 cells exposed to 20% or 1% O<sub>2</sub> for 16 h (Fig. 4 and Fig. S4). Antibodies against HIF-1 $\alpha$ , HIF-2 $\alpha$ , or HIF-1 $\beta$  and rabbit Ig (IgG) were used for ChIP. Three HIF binding sites were identified in the *RHOA* gene. Site 1 was located 1.1 kb 5' to the transcription start site (Fig. 4A) and showed significant hypoxia-induced binding of HIF-1 $\alpha$  and HIF-1 $\beta$  but not HIF-2 $\alpha$  (Fig. 4B). Two additional HIF binding sites were identified in intron 1 of *RHOA*. Site 2 also showed hypoxia-induced binding of HIF-1 $\alpha$  and HIF-1 $\beta$  but not HIF-2 $\alpha$ . Site 3 contained two matches to the consensus sequence within ~90 bp of each other that were



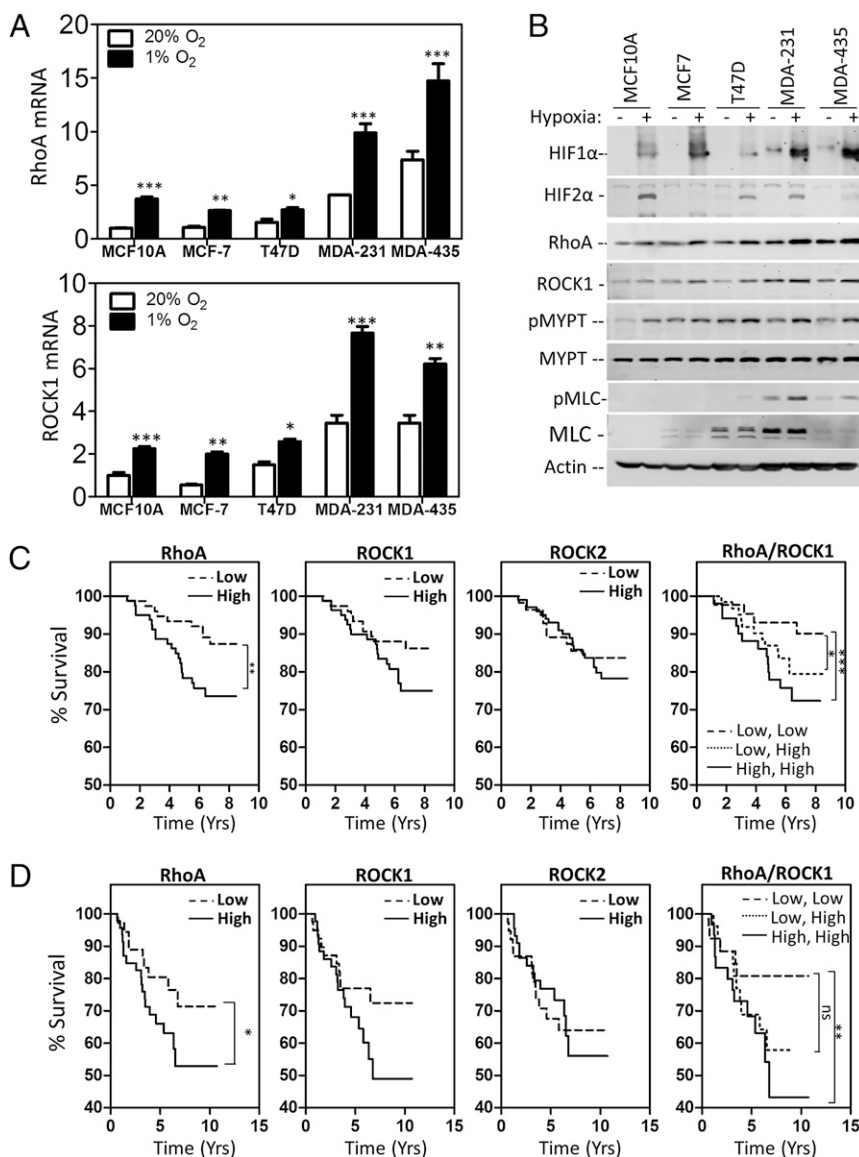


**Fig. 2.** Hypoxia induces RhoA and ROCK1 expression and MLC phosphorylation. (A) qRT-PCR was performed to quantify RhoA (Upper) and ROCK1 (Lower) mRNA levels in breast cell lines following exposure to 20% or 1% O<sub>2</sub> for 24 h. Data are shown as mean  $\pm$  SEM;  $n = 3$ . \* $P < 0.05$ , \*\* $P < 0.01$ , \*\*\* $P < 0.001$  vs. 20% O<sub>2</sub> (Student's  $t$  test). For each sample, the expression of RhoA or ROCK1 mRNA was quantified relative to 18S rRNA and then normalized to the result obtained from MCF-10A cells at 20% O<sub>2</sub>. Statistical analysis was performed before normalization. (B) Immunoblot assays were performed to quantify HIF-1 $\alpha$ , HIF-2 $\alpha$ , total RhoA, ROCK1, MYPT, MLC, pMYPT<sup>T853</sup>, and pMLC<sup>S19</sup> protein levels in breast cell lines following exposure to 20% O<sub>2</sub> (–) or 1% O<sub>2</sub> (+) for 48 h. (C and D) Kaplan-Meier analysis of disease-specific survival for breast cancer patients stratified by RhoA, ROCK1, ROCK2, or combined RhoA and ROCK1 mRNA expression in a 159-patient data set (40) (C) and an 82-patient data set (41) (D). Low = patients with mRNA levels less than the median. High = patients with mRNA levels greater than the median. Low, Low = patients with RhoA and ROCK1 mRNA levels less than the median. Low, High = patients with RhoA or ROCK1 mRNA greater than the median and the other mRNA less than the median. High, High = patients with RhoA and ROCK1 mRNA levels greater than the median. A Wilcoxon rank sum test was used to compare survival curves. \* $P < 0.05$ ; \*\* $P < 0.01$ ; \*\*\* $P < 0.001$ ; ns, not significant.

analyzed in the same PCR amplifier, which revealed significant hypoxia-induced binding of HIF-2 $\alpha$  and HIF-1 $\beta$  but not HIF-1 $\alpha$ . Thus, HIF-1 and HIF-2 bind to distinct sites in the *RHOA* gene in hypoxic breast cancer cells.

Three HIF binding sites also were identified in the *ROCK1* gene (Fig. 4 C and D). Site 1, located in intron 1, showed hypoxia-inducible binding of HIF-1 $\alpha$ , HIF-2 $\alpha$ , and HIF-1 $\beta$ . Site 2, located in intron 27, bound HIF-1 $\alpha$  and HIF-1 $\beta$  but not HIF-2 $\alpha$ . Site 3, located in intron 32, bound HIF-1 $\alpha$ , HIF-2 $\alpha$ , and HIF-1 $\beta$  (Fig. 4D). Taken together, the data presented in Fig. 4 demonstrate that HIF-1 and HIF-2 bind directly to multiple sites in the *RHOA* and *ROCK1* genes in hypoxic breast cancer cells, as is consistent with the coordinate regulation of *RHOA* and *ROCK1* expression observed in vitro and in vivo (Fig. 2) and the inhibitory effects of HIF-1 $\alpha$  and HIF-2 $\alpha$  knockdown on *RHOA* and *ROCK1* expression (Fig. 3A).

**HIFs Mediate the Formation of Stress Fibers and Focal Adhesions.** To determine if enhanced RhoA signaling under hypoxic conditions is sufficient to promote the formation of focal adhesions, MDA-MB-231 cells exposed to 20% or 1% O<sub>2</sub> for 24 h were stained with FITC-conjugated phalloidin to detect polymerized actin

(F-actin; green) and with anti-vinculin primary antibody with rhodamine-conjugated secondary antibody to detect focal adhesions (red) by fluorescence microscopy (Fig. 5A). Both actin polymerization/stress fiber formation and focal adhesion formation were enhanced under hypoxic conditions (Fig. 5B).

FAK activation, as measured by phosphorylation at T397 (pFAK<sup>T397</sup>), also was increased under hypoxic conditions, regardless of the ECM protein used as substratum (Fig. 5C and Fig. S5A). Analysis of pFAK<sup>T397</sup> in a panel of breast cell lines revealed that, although total FAK protein levels were not related to disease progression, pFAK<sup>T397</sup> levels were correlated with metastatic potential and pMLC status (compare Fig. 5D with Fig. 2B). Total FAK protein levels were not altered by hypoxia or HIF knockdown, but both HIF-1 $\alpha$  and HIF-2 $\alpha$  were required for enhanced pFAK<sup>T397</sup> levels under hypoxic conditions in MDA-MB-231 cells (Fig. 5E and F). Enhanced pFAK<sup>T397</sup> was associated with an increase in focal adhesion density and size in a HIF-dependent manner under hypoxic conditions (Fig. 5G and Fig. S5B). Treatment of MDA-MB-231 cells with the ROCK1 inhibitor Y-27632 blocked hypoxia-induced FAK<sup>T397</sup> phosphorylation (Fig. 5H). Based on the data presented in Fig. 5, we conclude that HIF-dependent induction of *RHOA* and *ROCK1* expression caused increased formation

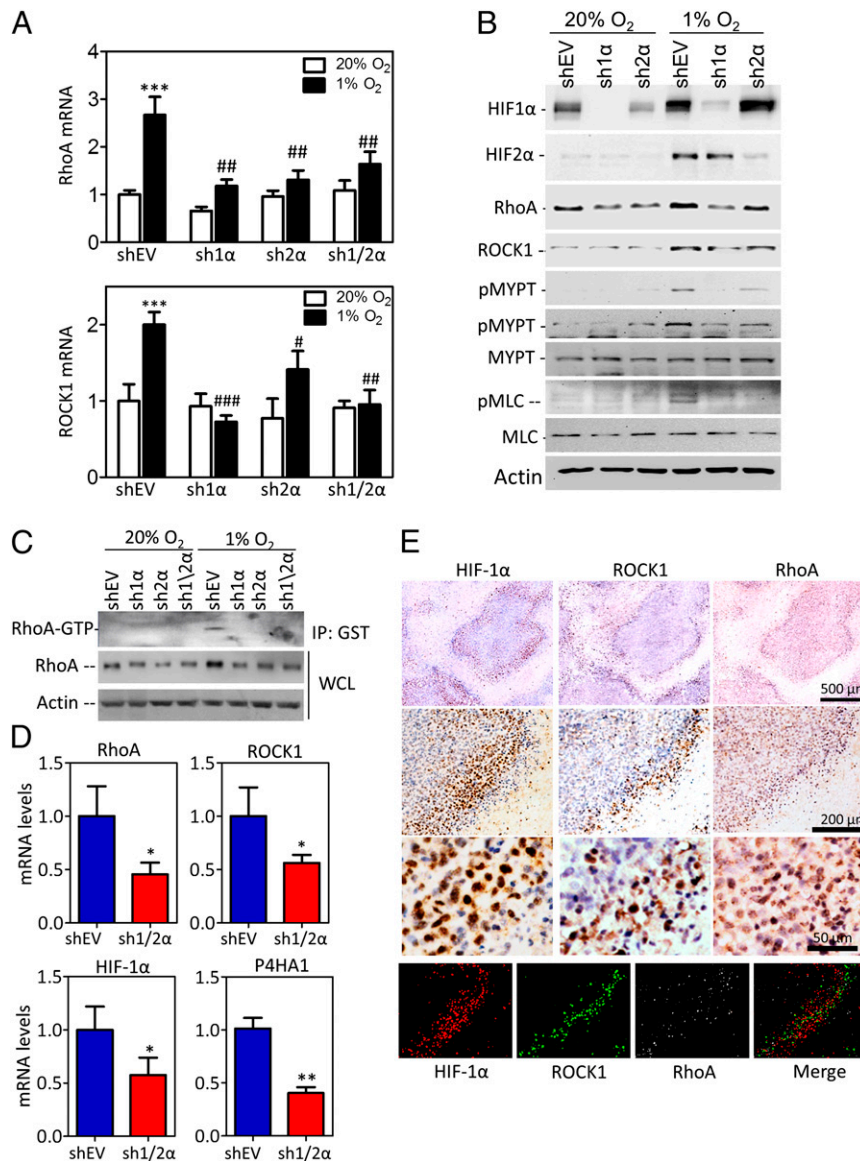


**Fig. 3.** Hypoxia-induced expression of RhoA and ROCK1 is HIF dependent. (A) qRT-PCR was performed to quantify RhoA (Upper) and ROCK1 (Lower) mRNA levels in MDA-MB-231 subclones exposed to 20% or 1% O<sub>2</sub> for 24 h. Data are shown as mean ± SEM; *n* = 3. \*\*\**P* < 0.001 vs. shEV cells at 20% O<sub>2</sub>; #*P* < 0.05, ##*P* < 0.01, ###*P* < 0.001 vs. shEV cells at 1% O<sub>2</sub> (two-way ANOVA with Bonferroni posttest). (B) Immunoblot assays were performed to quantify total RhoA, ROCK1, MYPT, MLC, pMYPT<sup>T853</sup> (pMYPT, Upper), pMYPT<sup>T696</sup> (pMYPT, Lower), and pMLC<sup>S19</sup> protein levels in cells exposed to 20% or 1% O<sub>2</sub> for 48 h. (C) Cells were exposed to 20% or 1% O<sub>2</sub> for 24 h, and whole-cell lysates (WCL) were incubated with GST-Rhotekin fusion protein, which interacts only with GTP-bound RhoA, and glutathione agarose beads. GTP-bound RhoA was eluted and analyzed by immunoblot assay. RhoA and actin levels in the input whole-cell lysate also were determined. (D and E) MDA-MB-231 subclones were injected into the mammary fat pad of SCID mice. Tumors were harvested on day 52. (D) qRT-PCR was performed to quantify RhoA, ROCK1, P4HA1, and HIF-1α mRNA levels in shEV and sh1/2α tumors, and values were normalized to shEV. Data are shown as mean ± SEM; *n* = 5 mice. \**P* < 0.05, \*\**P* < 0.01 vs. shEV (Student's *t* test). (E) (Top Three Rows) Immunohistochemistry was performed to detect ROCK1, RhoA, and HIF-1α in MDA-MB-231 shEV serial tumor sections, which were imaged at increasing magnification as indicated. In the top row, fields were imaged in a 3 × 3 array, and the array was stitched to obtain a large view of the tumor section. (Bottom Row) Staining was pseudocolored and merged to show colocalization.

of focal adhesions leading to FAK activation in hypoxic breast cancer cells.

**Focal Adhesions Are Required for Enhanced Cell Motility Under Hypoxic Conditions.** Cell motility requires the transmission of force through focal adhesions, and focal adhesion size has been shown to correlate directly with cell velocity (44). Therefore, the effect of focal adhesions on cell velocity induced by hypoxia was investigated by generating MDA-MB-231 subclones stably transfected with shEV vector or a vector encoding either of two independent shRNAs targeting FAK (Fig. 6A). The formation of

focal adhesions was disrupted by FAK knockdown, as indicated by anti-vinculin immunofluorescence (Fig. 6B). The velocity of hypoxic cells during random migration on slides coated with type I collagen or fibronectin was reduced by FAK knockdown to levels similar to those of sh1/2α cells (Fig. 6C and Fig. S6A). The maximum displacement of FAK-knockdown cells also was reduced dramatically, to levels similar to those in sh1/2α cells (Fig. 6D and Fig. S6B).

To inhibit the formation of focal adhesions by a method independent of genetic or pharmacologic approaches, substrate stiffness was modulated using functionalized polyacrylamide

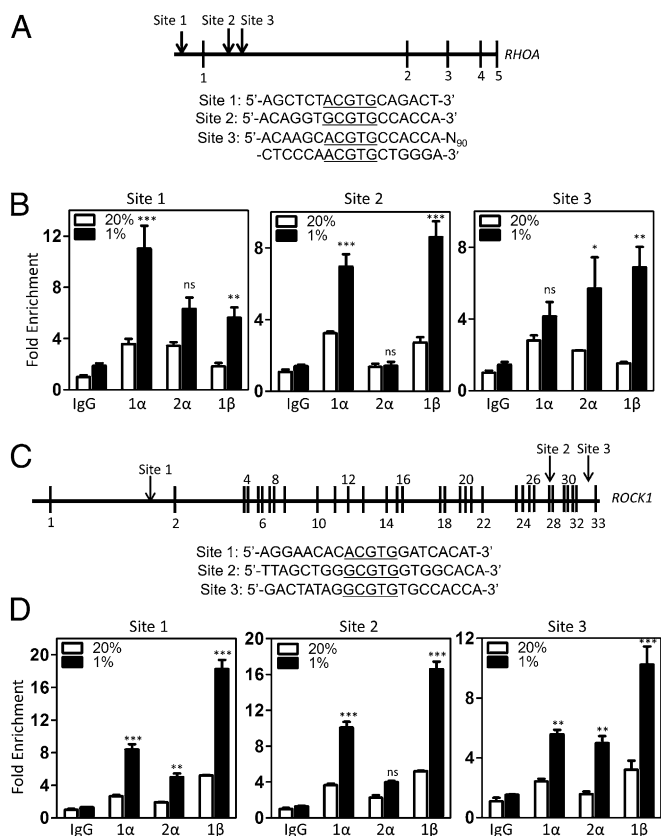


**Fig. 4.** HIF-1 and HIF-2 bind directly to the *RHOA* and *ROCK1* genes in hypoxic cells. (A) Three HIF binding sites in the 5'-flanking region and intron 1 of the human *RHOA* gene were identified by ChIP as described below. (B) MDA-MB-231 cells were incubated at 20% or 1% O<sub>2</sub> for 16 h, and ChIP assays were performed using IgG or antibodies against HIF-1 $\alpha$ , HIF-2 $\alpha$ , or HIF-1 $\beta$ . Primers flanking binding sites were used for qPCR, and values were normalized to cells exposed to 20% O<sub>2</sub> and ChIP with IgG. Data are shown as mean  $\pm$  SEM;  $n = 3$ . \* $P < 0.05$ , \*\* $P < 0.01$ , \*\*\* $P < 0.001$  vs. 20% O<sub>2</sub> (Student's  $t$  test). (C and D) HIF binding sites were identified in intron 1, intron 28, and intron 32 of the *ROCK1* gene (C) by ChIP (D), using the immunoprecipitates described above.

gels. As in glass and tissue culture dishes, incubating cells under hypoxia for 24 h on stiff polyacrylamide surfaces (>2,000 Pa) led to an increase in the formation of focal adhesions in shEV but not in sh1/2 $\alpha$  cells (Fig. 6E). Plating cells on a soft substratum (<200 Pa) blocked hypoxia-induced formation of focal adhesions, an effect similar to that seen with FAK or HIF knockdown. Similarly, cell velocity was enhanced by hypoxia on stiff but not on soft surfaces and required HIF activity (Fig. 6F). Taken together, the data presented in Fig. 6 demonstrate that the increased cell velocity that is induced by hypoxia in a HIF-dependent manner requires the formation of focal adhesions.

## Discussion

The results of this study show that hypoxia-induced, HIF-dependent coordinate transcriptional activation of the *RHOA* and *ROCK1* genes leads to pathway activation that is manifested by actin polymerization, MLC phosphorylation, actin-myosin cell contractility, cell-induced matrix contraction, and enhanced breast cancer cell motility (Fig. 7). Increased formation of focal adhesions and FAK phosphorylation, which also resulted from RhoA-ROCK1 activation, were required for enhanced cell motility under hypoxic conditions. Enhanced motility was abrogated by the knockdown of HIF-1 $\alpha$  and HIF-2 $\alpha$  or FAK or by inhibiting the formation of focal adhesions by plating cells on a soft substratum. Taken together,

these results delineate a molecular mechanism by which hypoxia, independent of genomic alterations, induces a signal-transduction pathway that triggers cytoskeletal reorganization, which underlies the motility of cancer cells and is an essential attribute of the invasive-metastatic phenotype.

**HIFs Mediate Enhanced Motility of Hypoxic Breast Cancer Cells.** In this study we dynamically evaluated the role of HIFs and chronic hypoxia in breast cancer cell motility. No change in cell motility was observed during the first 14 h of incubation at 1% O<sub>2</sub>, but cell motility increased during the last 8 h of observation. HIFs are induced rapidly upon exposure to 1% O<sub>2</sub>, and the delayed effect of hypoxia reflects the time required to induce signaling to the FAK pathway via increased RhoA and ROCK1 mRNA and protein expression. Immunoblot assays of MDA-MB-231 lysates confirmed that RhoA and ROCK1 induction occurs at 12 h and is maintained through 48 h of hypoxic exposure. Our data indicate that HIF  $\rightarrow$  RhoA  $\rightarrow$  ROCK1 signaling is required to induce cell motility under conditions of chronic hypoxia similar to those experienced in vivo. Clinical studies have demonstrated that the median pO<sub>2</sub> in advanced breast cancers is 10 mmHg (~1.5% O<sub>2</sub>), compared with 65 mmHg (~9.5% O<sub>2</sub>) in normal breast tissue, and that breast cancers with pO<sub>2</sub> <10 mmHg are associated with increased risk of metastasis and patient mortality (45). Our immunohistochemical analysis revealed striking coexpression of HIF-1 $\alpha$ , RhoA, and ROCK1 protein within the perinecrotic region of orthotopic breast tumors, as is consistent with coordinate transcriptional regulation of *RHOA* and *ROCK1* by HIFs. The significant correlation of RhoA and ROCK1 mRNA levels with expression of other HIF target genes in >500 human breast cancers indicates that this observation is clinically relevant.

**Increased Stiffness Primes Tumors for Hypoxic Induction of FAK Phosphorylation.** Women with dense breast tissue have an increased risk of breast cancer (46, 47). Tumor fibrosis promotes tumor stiffness, which in turn promotes cancer progression via FAK activation (48, 49). This study compared cells plated on a soft substratum mimicking normal breast tissue and cells plated on a stiff substratum that more closely resembled breast cancer tissue (49). The formation of focal adhesions, FAK phosphorylation, and cell motility were enhanced on the stiff substratum as compared with soft substratum, and this effect of substrate stiffness was dependent upon HIF activity. Thus, ECM stiffness and hypoxia synergistically activate RhoA  $\rightarrow$  ROCK1  $\rightarrow$  FAK signaling that is required for breast cancer cell motility and invasion.

**Levels of HIF-1 $\alpha$ , RhoA, and ROCK1 Correlate with Metastatic Status.** Our results show that HIF-1 $\alpha$ , RhoA, and ROCK1 are coexpressed in breast cell lines and cancer tissue. Expression was lowest in the nontransformed mammary epithelial cell line (MCF-10A) and highest in the metastatic breast cancer cell lines (MDA-MB-231 and MDA-MB-435). HIF-1 $\alpha$  expression in breast cancer is associated with decreased survival in multiple studies (30–33). In this study, decreased metastasis-free survival was predicted by RhoA and ROCK1 co-overexpression, with remarkably consistent results between two independent patient cohorts. The finding that ROCK1 mRNA overexpression significantly impacted mortality only in the context of RhoA mRNA overexpression is consistent with the role of RhoA as an obligate activator of ROCK1. Inhibition of HIF, RhoA, or ROCK1 expression using RNA interference in MDA-MB-231 cells has been shown to impair metastasis significantly (16, 18, 29). Likewise, targeting either HIF or ROCK1 pharmacologically abrogates metastasis in animal models (18, 29, 37, 39, 50).



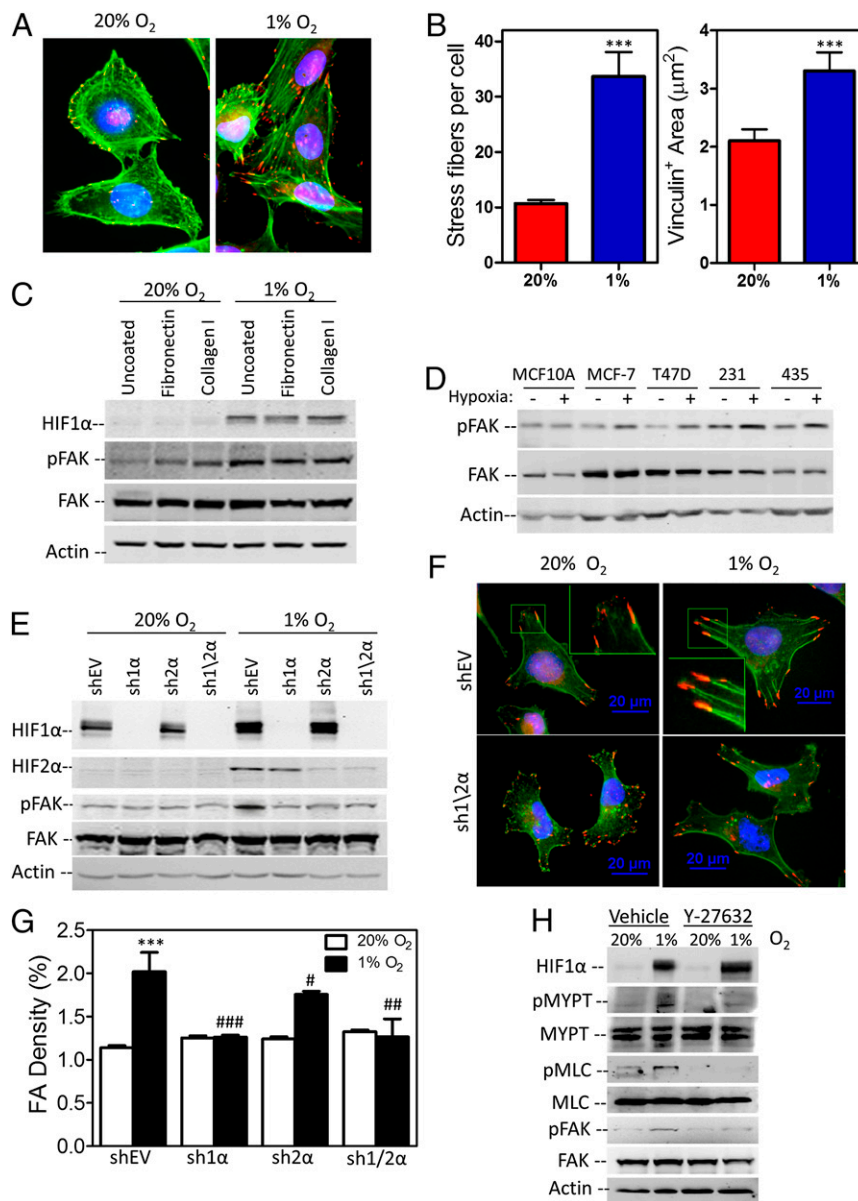


**Fig. 5.** RhoA/ROCK1 signaling stimulates the formation of focal adhesions in hypoxic cells. (A) MDA-MB-231 cells were exposed to 20% or 1% O<sub>2</sub> for 24 h and were stained with FITC-phalloidin to detect F-actin stress fibers (green), with anti-vinculin antibodies to detect focal adhesions (red), and with DAPI, to detect nuclei (blue). (B) (Left) The number of stress fibers per cell was quantified based on F-actin staining. Data are shown as mean ± SEM; n = 50 cells. \*\*\*P < 0.001 vs. 20% O<sub>2</sub> (Student's *t* test). (Right) The focal adhesion area was determined based on vinculin staining. Data are shown as mean ± SEM; n = 50 cells. \*\*\*P < 0.001 vs. 20% O<sub>2</sub> (Student's *t* test). (C) Immunoblot assays were performed to quantify levels of HIF-1α, pFAK<sup>T397</sup>, and total FAK protein levels in MDA-MB-231 cells cultured on uncoated, fibronectin-coated, or type I collagen-coated plates and exposed to 20% or 1% O<sub>2</sub> for 24 h. (D and E) Immunoblot assays were performed to quantify pFAK<sup>T397</sup> and total FAK in breast cell lines (D) and MDA-MB-231 subclones (E) following exposure to 20% or 1% O<sub>2</sub> for 24 h. (F) MDA-MB-231 subclones were exposed to 20% or 1% O<sub>2</sub> for 24 h and were stained with FITC-phalloidin (F-actin; green), anti-pFAK<sup>T397</sup> (focal adhesions; red), and DAPI (nuclei; blue). (G) Image analysis was performed to determine the focal adhesion (FA) density per cell. Data are shown as mean ± SEM; n = 50 cells. \*\*\*P < 0.001 vs. shEV cells at 20% O<sub>2</sub>; #P < 0.05, ###P < 0.01, ####P < 0.001 vs. shEV cells at 1% O<sub>2</sub> (two-way ANOVA with Bonferroni posttest). (H) Immunoblot assays were performed for HIF-1α, pMYPT<sup>T853</sup>, total MYPT, pMLC<sup>S19</sup>, total MLC, pFAK<sup>T397</sup>, and total FAK protein levels in MDA-MB-231 cells treated with vehicle or the ROCK inhibitor Y-27632 during exposure to 20% or 1% O<sub>2</sub> for 24 h.

**FAK Activity, but Not FAK Expression, Is Increased in Metastatic Breast Cancer Cells.** Our results demonstrate that FAK is a major effector of RhoA/ROCK1 in hypoxic breast cancer cells. Interestingly, total levels of FAK or MLC protein did not correlate with metastatic potential in the mammary cell lines investigated. This result is supported by studies showing that a large fraction of breast cancers, as well as preinvasive ductal carcinomas in situ, express elevated FAK protein levels and that

the FAK activation state is more informative than total protein levels (51). These findings in breast cancer are in contrast to those in melanoma, in which HIF-dependent *FAK* gene transcription promotes invasion (52). Given that MLC and FAK protein levels are not limiting in breast cancer, our study suggests that FAK may be poised for activation by an hypoxic tumor microenvironment. In contrast, RhoA mRNA and protein levels varied with the metastatic potential of the mammary cell

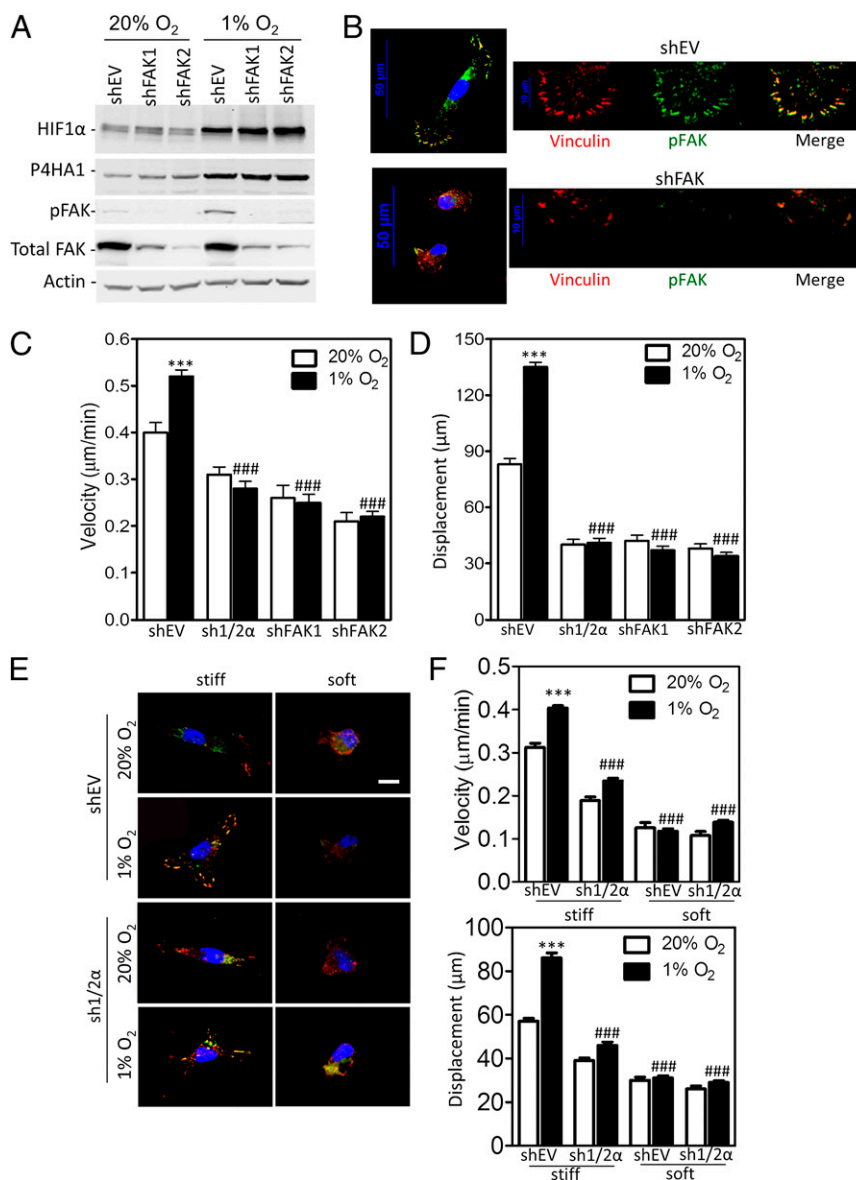


**Fig. 6.** Hypoxia-induced motility requires the formation of focal adhesions and FAK activity. (A) MDA-MB-231 subclones stably expressing either of two independent shRNAs against FAK (shFAK1 or shFAK2) were exposed to 20% or 1% O<sub>2</sub> for 24 h, and immunoblot assays were performed. (B) MDA-MB-231 subclones were exposed to 20% or 1% O<sub>2</sub> for 24 h and stained with antibodies against vinculin (red) and pFAK<sup>T397</sup> (green); colocalization (yellow) is observed in the merge image. A magnified view of the photomicrographs is shown on the left. (C) The velocity of subclones migrating on collagen-coated surfaces during 14–24 h of exposure to 20% or 1% O<sub>2</sub> was determined. Data are shown as mean ± SEM; *n* = 50. \*\*\**P* < 0.001 vs. shEV cells at 20% O<sub>2</sub>; ###*P* < 0.001 vs. shEV cells at 1% O<sub>2</sub> (two-way ANOVA with Bonferroni posttest). (D) The maximum displacement of each cell was determined and is shown as mean ± SEM, *n* = 50. \*\*\**P* < 0.001 vs. shEV cells at 20% O<sub>2</sub>; ###*P* < 0.001 vs. shEV cells at 1% O<sub>2</sub> (two-way ANOVA with Bonferroni posttest). (E) Vinculin (red) and pFAK<sup>T397</sup> (green) were detected by immunofluorescence in MDA-MB-231 cells plated on soft or stiff polyacrylamide gels following exposure to 20% or 1% O<sub>2</sub> for 16 h. (F) Velocity (Upper) and maximum displacement (Lower) of MDA-MB-231 cells migrating on soft or stiff surfaces during 14–24 h of exposure to 20% or 1% O<sub>2</sub> were determined. Data are shown as mean ± SEM; *n* = 50. \*\*\**P* < 0.001 vs. shEV on the stiff surface at 20% O<sub>2</sub>; ###*P* < 0.001 vs. shEV cells on the stiff surface at 1% O<sub>2</sub> (two-way ANOVA with Bonferroni posttest).

lines, and increased RhoA levels under hypoxic conditions were associated with activation of ROCK1; increased expression of ROCK1 also was induced by hypoxia in an HIF-dependent manner.

**Therapeutic Implications.** Both of the metastatic cell lines studied were derived from triple-negative breast cancers, which do not express estrogen, progesterone, or HER2 receptors, respond poorly to chemotherapy (53), and are characterized by increased expression of the HIF transcriptome (42). Because Rho/Rock/FAK signaling is potentially activated by HIFs under hypoxia, treatment protocols that use FAK or HIF inhibitors (54, 55) may

be especially beneficial for breast cancer patients with high HIF levels in their primary tumors.

## Materials and Methods

**Cell Lines and Culture.** Breast cancer cell lines MCF-7, T47D, MDA-MB-231, and MDA-MB-435 (provenance is reviewed in ref. 56) and human foreskin fibroblasts were maintained in high-glucose (4.5 mg/mL) DMEM supplemented with 10% (vol/vol) FBS and 1% penicillin-streptomycin (Invitrogen). MCF-10A cells were maintained as described (57). All cells were maintained at 37 °C in a 5% CO<sub>2</sub>, 95% air incubator. Hypoxic cells were maintained at 37 °C in a modular incubator chamber (Billups-Rothenberg) flushed with a gas mixture containing 1% O<sub>2</sub>, 5% CO<sub>2</sub>, and 94% N<sub>2</sub>.



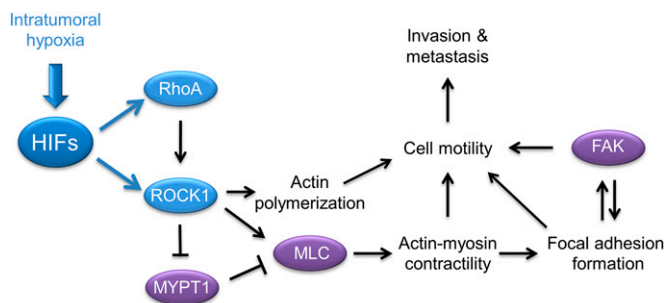


**Fig. 7.** Consequences of coordinate activation of *RHOA* and *ROCK1* by HIFs. Schematic diagram of hypoxia-induced and HIF-regulated RhoA/ROCK1 expression, which inhibits MYPT activity and increases MLC phosphorylation, leading to actin polymerization, cell motility, actin-myosin contractility, and the formation of focal adhesions which promote FAK activation. The pathways converge to promote cell motility, an essential step required for invasion and metastasis. Results from this study show that hypoxia promotes motility through the RhoA → ROCK1 signaling pathway. Blue: transcriptional regulation. Black: signaling mechanisms.

**shRNA, Lentiviruses, and Transduction.** Expression vectors encoding shRNA targeting HIF-1 $\alpha$  and HIF2 $\alpha$  (29) and FAK (9) were described previously. Lentiviruses were packaged in 293T cells by cotransfection with plasmid pCMV-dR8.91 and plasmid encoding vesicular stomatitis virus G protein using Lipofectamine 2000 (Invitrogen). Medium containing viral particles was collected 48 h after transfection and passed through a 0.45- $\mu$ m filter. MDA-MB-231 cells and fibroblasts were transduced with viral supernatant supplemented with 8  $\mu$ g/mL Polybrene (Sigma-Aldrich). After 24 h, cells were maintained in medium containing 0.6  $\mu$ g/mL puromycin (Sigma-Aldrich).

**Immunohistochemistry.** Tumors were fixed in 10% formalin and were embedded in paraffin. Sections were dewaxed with xylene and hydrated with graded ethanols, followed by antigen retrieval using citrate buffer (pH 6.1). Immunohistochemistry was performed using the LSAB+ System HRP kit (DAKO) and RhoA or ROCK1 antibodies (Novus Biologicals). HIF-1 $\alpha$  immunohistochemistry was performed as described (58).

**ChIP.** MDA-MB-231 cells were exposed to 20% or 1% O<sub>2</sub> for 16 h and crosslinked in the presence of 3.7% formaldehyde for 10 min. Immunoprecipitation with HIF-1 $\alpha$  (Santa Cruz), HIF-2 $\alpha$ , HIF-1 $\beta$ , or IgG antibodies (Novus Biologicals) was performed overnight. DNA was purified by phenol-chloroform extraction and ethanol precipitation. Candidate binding sites were analyzed by qPCR using primers that flanked the candidate HIF binding site sequences. Primer sequences are as follows: *RHOA* site 1: CCTATCCTA-CAGGCTGCTGAA and TAAGCCACCAGCTTAATGG; *RHOA* site 2: GATG-GAGTCTCGCTCTGCA and CAAGGGGGTAAAGAAATAAAGCA; *RHOA* site 3: AAGTATTCCCTGCTCA and GCAACAGAGCGAGATTCCAT; *ROCK1* site 1: AACACAGGGTCTTGCTCT and AAGGTTCTCCTCTCTTTC; *ROCK1* site 2: CCCTTACACCGGGCGT and CTGGTTGAAGCAATTCCCC; *ROCK1* site 3: CCTCTGAGTAGCTGGGACT and GAGTTGAAACCAGCCTGGA.

**Immunoblot Assays.** Aliquots of whole-cell lysates prepared in Nonidet P-40 buffer were fractionated by 8% or 15% (for RhoA and MLC, respectively) SDS/PAGE. Antibodies against the following proteins were used: HIF-1 $\alpha$  (BD Transduction Laboratory); HIF-2 $\alpha$ , pFAK<sup>T397</sup>, FAK, MYPT, ROCK1, and RhoA (Novus Biologicals); phosphorylated MYPT (pMYPT<sup>T853</sup>, pMYPT<sup>T696</sup>), MLC, and pMLC<sup>S19</sup> (Cell Signaling); and  $\beta$ -actin (Santa Cruz). HRP-conjugated secondary antibodies were purchased from Santa Cruz. The chemiluminescence signal was detected using ECL Plus (GE Healthcare).

**qRT-PCR.** RNA was extracted using TRIzol (Invitrogen) and treated with DNase I (Ambion). cDNA was synthesized with the iScript cDNA synthesis kit (Bio-Rad). qPCR was performed with SYBR Green qPCR master mix (Fermentas) using a Bio-Rad iCycler. The expression of each target mRNA relative to 18S rRNA was calculated based on the threshold cycle (C<sub>t</sub>) as  $2^{-\Delta(\Delta C_t)}$ , where  $\Delta C_t = C_t$  (target) - C<sub>t</sub> (18S) and  $\Delta(\Delta C_t) = \Delta C_t$  (control sample) -  $\Delta C_t$  (test sample). Primer sequences are as follows: ROCK1: AACATGCTGCTGGATAAATCTGG and TGTATCACATCGTACCATCGCT; 18S rRNA: GAGGATGAGGTGGAACGCTGT and AGAAGTGACGACAGCCTCTA; RhoA: CAGAAAAGTGGACCCAGAA and GCAGCTGCTCTCGTAGCCATTTC.

**Preparation of Collagen-Coated Culture Plates.** Cell-culture plates were coated with soluble rat tail type I collagen in acetic acid (BD Biosciences) to achieve a coverage of 33  $\mu$ g/cm<sup>2</sup> and were incubated at room temperature for 2 h. The 3.5-cm plates were washed gently three times with PBS and seeded with  $1 \times 10^4$  cells.

**Statistical Analysis of Microarray Data.** Level 3 data from the Breast Invasive Carcinoma dataset (42) were obtained from <http://tcga-data.nci.nih.gov/tcga/tcgaHome2.jsp>. Pearson's correlation coefficient was used to determine *P* values for coexpression. Prognostic significance of RhoA, ROCK1, and ROCK2 mRNA expression in breast cancer was examined in the Pawitan (GSE1456) (40) and Minn (GSE2603) (41) microarray datasets. Survival plots were created using Kaplan–Meier methods in GraphPad Prism Software.

**Cell Motility Measurements.** Cell velocity was determined by tracking single cells using image-recognition software (MetaMorph/Metavue). The change in

cell position was recorded every 10 min. Cell displacement,  $\sqrt{x(t)^2 + y(t)^2}$ , was calculated using the *x* and *y* coordinates (in micrometers) of each cell for each measurement recorded. The *x* and *y* coordinates of each cell were set to zero for the initial time point. Maximum displacement =  $\text{maximum}_{t=0}^{t=22 \text{ hr}} (\sqrt{x(t)^2 + y(t)^2})$ , where *t* = time.

**Immunofluorescence and Confocal Microscopy.** MDA-MB-231 cells were fixed with 4% paraformaldehyde (Sigma), permeabilized with 0.1% Triton X-100 (Fisher) for 5 min, and blocked with PBS supplemented with FBS (10%, vol/vol) for 20 min. For focal adhesion staining, vinculin (Sigma) and pFAK<sup>T397</sup> (Novus) antibodies were used. Actin filaments and nuclear DNA were stained using Alexa-Fluor 488-conjugated phalloidin and 300 nM DAPI, respectively (Invitrogen). Fluorescent imaging was performed by confocal laser microscopy (A1; Nikon) through a 60 $\times$  plan or water immersion lens (NA = 1.2). Images were analyzed and processed using MetaMorph (Molecular Devices) or NIS elements (Nikon). Morphometric analysis (area, perimeter, length) of focal adhesions was conducted using MetaMorph. GraphPad Prism (GraphPad Software) was used to calculate and plot mean and standard error of the mean (SEM) of measured quantities, and significance was assessed by two-way ANOVA.

**3D Type I Collagen Matrix for Contraction Assays.** Cells embedded in 3D collagen matrices were prepared by mixing cells suspended in cell-culture medium with 10 $\times$  collagen reconstitution buffer [2.2% (wt/vol) NaHCO<sub>3</sub>, 0.05 N NaOH, and 200 mM HEPES] and soluble rat tail type I collagen in acetic acid (BD Biosciences) to achieve a final concentration of 2 mg/mL collagen. Gels were solidified at 37  $^{\circ}$ C.

**Preparation of Polyacrylamide Substrates.** Polyacrylamide substrates were prepared on 12-well glass-bottomed dishes (MatTek Corporation). Stiff or soft gels were prepared by mixing 0.175% (stiff) or 0.0175% (soft) *N,N*-methylenebisacrylamide and 7.5% acrylamide in distilled H<sub>2</sub>O and were crosslinked by the addition of 0.01% (wt/vol) ammonium persulfate and 0.001% (vol/vol) *N,N,N',N'*-tetramethylethylenediamine (Invitrogen). A coverslip was placed over the droplets to ensure the formation of a flat gel surface after polymerization. The UV-activated bifunctional cross-linker sulfo-succinimidyl hexanoate (Pierce) was used to couple 10  $\mu$ g/mL of fibronectin or collagen to the gel surface.

**RhoA Activation Assay.** GTP-bound RhoA was quantified as previously described (59). MDA-MB-231 cells were lysed with RIPA buffer [50 mM Tris (pH 7.2), 500 mM NaCl, 1% Triton X-100, 0.5% sodium deoxycholate, 1% SDS, 10 mM MgCl<sub>2</sub>, 0.5  $\mu$ g/mL leupeptin, 0.7  $\mu$ g/mL pepstatin, 4  $\mu$ g/mL aprotinin, and 2 mM PMSF]. After centrifugation at 14,000  $\times$  g for 3 min, the lysate was incubated with bacterially expressed and purified GST-Rhotekin Rho-binding domain fusion protein (59) bound to glutathione beads for 1 h at 4  $^{\circ}$ C. The beads were washed three times with Tris buffer (pH 7.2) containing 1% Triton X-100, 150 mM NaCl, and 10 mM MgCl<sub>2</sub>. RhoA protein levels were determined by immunoblot assay using anti-RhoA antibody (Novus Biologicals).

**ACKNOWLEDGMENTS.** We thank Karen Padgett of Novus Biologicals for providing IgG, FAK, HIF-1 $\beta$ , HIF-2 $\alpha$ , MYPT, pFAK<sup>T397</sup>, RhoA, and ROCK1 antibodies. This work was supported by National Cancer Institute Grant U54-CA143868 and the Johns Hopkins Institute for Cell Engineering. G.L.S. is the C. Michael Armstrong Professor at The Johns Hopkins University School of Medicine and is an American Cancer Society Research Professor. D.M.G. is the recipient of a Susan G. Komen Breast Cancer Foundation Postdoctoral Fellowship Award. S.J.L. is the recipient of a Provost's Award from The Johns Hopkins University.

1. Jaffe AB, Hall A (2005) Rho GTPases: Biochemistry and biology. *Annu Rev Cell Dev Biol* 21:247–269.
2. Narumiya S, Tanji M, Ishizaki T (2009) Rho signaling, ROCK and mDia1, in transformation, metastasis and invasion. *Cancer Metastasis Rev* 28(1-2):65–76.
3. Olson MF, Sahai E (2009) The actin cytoskeleton in cancer cell motility. *Clin Exp Metastasis* 26(4):273–287.
4. Jacobs M, et al. (2006) The structure of dimeric ROCK I reveals the mechanism for ligand selectivity. *J Biol Chem* 281(1):260–268.
5. Amano M, et al. (1996) Phosphorylation and activation of myosin by Rho-associated kinase (Rho-kinase). *J Biol Chem* 271(34):20246–20249.
6. Kimura K, et al. (1996) Regulation of myosin phosphatase by Rho and Rho-associated kinase (Rho-kinase). *Science* 273(5272):245–248.
7. Maekawa M, et al. (1999) Signaling from Rho to the actin cytoskeleton through protein kinases ROCK and LIM-kinase. *Science* 285(5429):895–898.
8. Plotnikov SV, Waterman CM (2013) Guiding cell migration by tugging. *Curr Opin Cell Biol* 25(5):619–626.
9. Fraley SL, et al. (2010) A distinctive role for focal adhesion proteins in three-dimensional cell motility. *Nat Cell Biol* 12(6):598–604.
10. Mitra SK, Hanson DA, Schlaepfer DD (2005) Focal adhesion kinase: In command and control of cell motility. *Nat Rev Mol Cell Biol* 6(1):56–68.
11. Provenzano PP, Inman DR, Eliceiri KW, Keely PJ (2009) Matrix density-induced mechanoregulation of breast cell phenotype, signaling and gene expression through a FAK-ERK linkage. *Oncogene* 28(49):4326–4343.
12. Luo M, et al. (2009) Mammary epithelial-specific ablation of the focal adhesion kinase suppresses mammary tumorigenesis by affecting mammary cancer stem/progenitor cells. *Cancer Res* 69(2):466–474.
13. Mitra SK, Lim ST, Chi A, Schlaepfer DD (2006) Intrinsic focal adhesion kinase activity controls orthotopic breast carcinoma metastasis via the regulation of urokinase plasminogen activator expression in a syngeneic tumor model. *Oncogene* 25(32):4429–4440.
14. Wang W, et al. (2004) Identification and testing of a gene expression signature of invasive carcinoma cells within primary mammary tumors. *Cancer Res* 64(23):8585–8594.
15. Bellizzi A, et al. (2008) RhoA protein expression in primary breast cancers and matched lymphocytes is associated with progression of the disease. *Int J Mol Med* 22(1):25–31.
16. Chan CH, et al. (2010) Deciphering the transcriptional complex critical for RhoA gene expression and cancer metastasis. *Nat Cell Biol* 12(5):457–467.
17. Lane J, Martin TA, Watkins G, Mansel RE, Jiang WG (2008) The expression and prognostic value of ROCK I and ROCK II and their role in human breast cancer. *Int J Oncol* 33(3):585–593.
18. Liu S, Goldstein RH, Scepansky EM, Rosenblatt M (2009) Inhibition of rho-associated kinase signaling prevents breast cancer metastasis to human bone. *Cancer Res* 69(22):8742–8751.
19. Ma L, et al. (2010) Over expression of RhoA is associated with progression in invasive breast duct carcinoma. *Breast J* 16(1):105–107.
20. Brahimi-Horn MC, Chiche J, Pouyssegur J (2007) Hypoxia and cancer. *J Mol Med (Berl)* 85(12):1301–1307.
21. Gillies RJ, Gatenby RA (2007) Hypoxia and adaptive landscapes in the evolution of carcinogenesis. *Cancer Metastasis Rev* 26(2):311–317.
22. Sullivan R, Graham CH (2007) Hypoxia-driven selection of the metastatic phenotype. *Cancer Metastasis Rev* 26(2):319–331.
23. Vaupel P, Höckel M, Mayer A (2007) Detection and characterization of tumor hypoxia using pO<sub>2</sub> histography. *Antioxid Redox Signal* 9(8):1221–1235.
24. Semenza GL (2010) Defining the role of hypoxia-inducible factor 1 in cancer biology and therapeutics. *Oncogene* 29(5):625–634.
25. Gilkes DM, et al. (2013) Collagen prolyl hydroxylases are essential for breast cancer metastasis. *Cancer Res* 73(11):3285–3296.
26. Gilkes DM, et al. (2013) Procollagen lysyl hydroxylase 2 is essential for hypoxia-induced breast cancer metastasis. *Mol Cancer Res* 11(5):456–466.
27. Chaturvedi P, et al.; Kshitz (2013) Hypoxia-inducible factor-dependent breast cancer-mesenchymal stem cell bidirectional signaling promotes metastasis. *J Clin Invest* 123(1):189–205.
28. Wong CC, et al. (2011) Hypoxia-inducible factor 1 is a master regulator of breast cancer metastatic niche formation. *Proc Natl Acad Sci USA* 108(39):16369–16374.
29. Zhang H, et al. (2012) HIF-1-dependent expression of angiotensin-like 4 and L1CAM mediates vascular metastasis of hypoxic breast cancer cells to the lungs. *Oncogene* 31(14):1757–1770.
30. Bos R, et al. (2003) Levels of hypoxia-inducible factor-1 $\alpha$  independently predict prognosis in patients with lymph node negative breast carcinoma. *Cancer* 97(6):1573–1581.
31. Dales JP, et al. (2005) Overexpression of hypoxia-inducible factor HIF-1 $\alpha$  predicts early relapse in breast cancer: Retrospective study in a series of 745 patients. *Int J Cancer* 116(5):734–739.
32. Generali D, et al. (2006) Hypoxia-inducible factor-1 $\alpha$  expression predicts a poor response to primary chemoendocrine therapy and disease-free survival in primary human breast cancer. *Clin Cancer Res* 12(15):4562–4568.
33. Schindl M, et al.; Austrian Breast and Colorectal Cancer Study Group (2002) Overexpression of hypoxia-inducible factor 1 $\alpha$  is associated with an unfavorable prognosis in lymph node-positive breast cancer. *Clin Cancer Res* 8(6):1831–1837.
34. Helczynska K, et al. (2008) Hypoxia-inducible factor-2 $\alpha$  correlates to distant recurrence and poor outcome in invasive breast cancer. *Cancer Res* 68(22):9212–9220.
35. Wells A, Grahovac J, Wheeler S, Ma B, Lauffenburger D (2013) Targeting tumor cell motility as a strategy against invasion and metastasis. *Trends Pharmacol Sci* 34(5):283–289.
36. Ginis I, Faller DV (2000) Hypoxia affects tumor cell invasiveness in vitro: The role of hypoxia-activated ligand HAL1/13 (Ku86 autoantigen). *Cancer Lett* 154(2):163–174.
37. Schito L, et al. (2012) Hypoxia-inducible factor 1-dependent expression of platelet-derived growth factor B promotes lymphatic metastasis of hypoxic breast cancer cells. *Proc Natl Acad Sci USA* 109(40):E2707–E2716.
38. Ridley AJ, et al. (2003) Cell migration: Integrating signals from front to back. *Science* 302(5651):1704–1709.
39. Itoh K, et al. (1999) An essential part for Rho-associated kinase in the transcellular invasion of tumor cells. *Nat Med* 5(2):221–225.
40. Pawitan Y, et al. (2005) Gene expression profiling spares early breast cancer patients from adjuvant therapy: Derived and validated in two population-based cohorts. *Breast Cancer Res* 7(6):R953–R964.
41. Minn AJ, et al. (2005) Genes that mediate breast cancer metastasis to lung. *Nature* 436(7050):518–524.
42. Cancer Genome Atlas Network (2012) Comprehensive molecular portraits of human breast tumours. *Nature* 490(7418):61–70.
43. Semenza GL, et al. (1996) Hypoxia response elements in the aldolase A, enolase 1, and lactate dehydrogenase A gene promoters contain essential binding sites for hypoxia-inducible factor 1. *J Biol Chem* 271(51):32529–32537.
44. Kim DH, Wirtz D (2013) Predicting how cells spread and migrate: Focal adhesion site does matter. *Cell Adhes Migr* 7(3):293–296.
45. Vaupel P, Mayer A, Höckel M (2004) Tumor hypoxia and malignant progression. *Methods Enzymol* 381:335–354.
46. Martin LJ, Boyd NF (2008) Mammographic density. Potential mechanisms of breast cancer risk associated with mammographic density: Hypotheses based on epidemiological evidence. *Breast Cancer Res* 10(1):201.
47. Provenzano PP, et al. (2008) Collagen density promotes mammary tumor initiation and progression. *BMC Med* 6:11.
48. Levental KR, et al. (2009) Matrix crosslinking forces tumor progression by enhancing integrin signaling. *Cell* 139(5):891–906.
49. Paszek MJ, et al. (2005) Tensional homeostasis and the malignant phenotype. *Cancer Cell* 8(3):241–254.
50. Wong CC, et al. (2012) Inhibitors of hypoxia-inducible factor 1 block breast cancer metastatic niche formation and lung metastasis. *J Mol Med (Berl)* 90(7):803–815.
51. Madan R, Smolkin MB, Cocker R, Fayyad R, Oktay MH (2006) Focal adhesion proteins as markers of malignant transformation and prognostic indicators in breast carcinoma. *Hum Pathol* 37(1):9–15.
52. Hanna SC, et al. (2013) HIF1 $\alpha$  and HIF2 $\alpha$  independently activate SRC to promote melanoma metastases. *J Clin Invest* 123(5):2078–2093.
53. Perou CM, et al. (2000) Molecular portraits of human breast tumours. *Nature* 406(6797):747–752.
54. Infante JR, et al. (2012) Safety, pharmacokinetic, and pharmacodynamic phase I dose-escalation trial of PF-00562271, an inhibitor of focal adhesion kinase, in advanced solid tumors. *J Clin Oncol* 30(13):1527–1533.
55. Kummar S, et al. (2011) Multihistology, target-driven pilot trial of oral topotecan as an inhibitor of hypoxia-inducible factor-1 $\alpha$  in advanced solid tumors. *Clin Cancer Res* 17(15):5123–5131.
56. Chambers AF (2009) MDA-MB-435 and M14 cell lines: Identical but not M14 melanoma? *Cancer Res* 69(13):5292–5293.
57. Debnath J, Muthuswamy SK, Brugge JS (2003) Morphogenesis and oncogenesis of MCF-10A mammary epithelial acini grown in three-dimensional basement membrane cultures. *Methods* 30(3):256–268.
58. Krishnamachary B, Semenza GL (2007) Analysis of hypoxia-inducible factor 1 $\alpha$  expression and its effects on invasion and metastasis. *Methods Enzymol* 435:347–354.
59. Ren XD, Kiosses WB, Schwartz MA (1999) Regulation of the small GTP-binding protein Rho by cell adhesion and the cytoskeleton. *EMBO J* 18(3):578–585.